
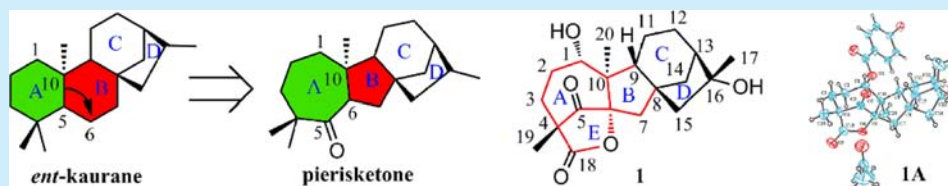


Pierisketolide A and Pierisketones B and C, Three Diterpenes with an Unusual Carbon Skeleton from the Roots of *Pieris formosa*

Chang-Shan Niu, Yong Li, Yun-Bao Liu, Shuang-Gang Ma, Fei Liu, Li Li, Song Xu, Xiao-Jing Wang, Ru-Bing Wang, Jing Qu,* and Shi-Shan Yu*

State Key Laboratory of Bioactive Substance and Function of Natural Medicines, Institute of Materia Medica, Chinese Academy of Medical Sciences and Peking Union Medical College, Beijing 100050, China

 Supporting Information



ABSTRACT: Pierisketolide A (1) and pierisketones B and C (2 and 3), three diterpenes with an unusual A-homo-B-nor-*ent*-kaurane carbon skeleton, were isolated from the roots of *Pieris formosa*. Their structures were characterized by a series of spectroscopic methods, X-ray diffraction, and electronic circular dichroism (ECD). Pierisketolide A (1) exhibited an analgesic effect with a 45% writhing inhibition rate at a dose of 10.0 mg/kg. The plausible biosynthetic pathways of 1–3 are proposed.

Terpenoids play an important role in natural product chemistry and biology.¹ As a large group of compounds, the *ent*-kaurane diterpenoids have attracted a great deal of attention due to their diverse structures and biological properties.² To date, thousands of *ent*-kauranoids with several novel skeletons³ have been isolated and characterized. Some display excellent antitumor⁴ and anti-inflammatory⁵ activities.

Pieris formosa (Wall) D.Don is a toxic shrub endemic to south and southwest China⁶ that has been used to treat tinea and scabies.⁷ As a rich source of terpenoids, numerous diterpenes, especially grayanoids (a special type of diterpenoid that exists exclusively in Ericaceae family), have been isolated from this plant. The biogenetic precursor for grayanane is assumed to be *ent*-kaurene.⁸ However, somewhat surprisingly, *ent*-kauranoids are rarely isolated from *P. formosa*. Previous phytochemical investigations of the stems of *P. formosa* have shown the presence of 15 grayananes.⁹ In our continuing endeavor to discover structurally diverse and biologically interesting metabolites from traditional Chinese medicines, three *ent*-kaurene-derived diterpenes, pierisketolide A (1) and pierisketones B–C (2 and 3) (see Figure 1), were isolated from the roots of *P. formosa*. Notably, 1–3 possessed an unusual A-homo-B-nor-*ent*-kaurane carbon skeleton with a pentacyclic 7/5/5/6/5 ring system (pierisketolide A, 1) and a tetracyclic 7/5/6/5 ring system (pierisketones B, 2 and C, 3). In this paper, we describe the isolation, structural elucidation, and bioactivity as well as the plausible biosynthetic pathways of pierisketolide A (1) and pierisketones B and C (2 and 3).

Pierisketolide A (1) was initially isolated as an amorphous power. The molecular formula C₂₀H₂₈O₅ with seven degrees of unsaturation was established by (+)-HRESIMS data (*m/z* 371.1823 [M + Na]⁺, calcd for 371.1829), in combination with

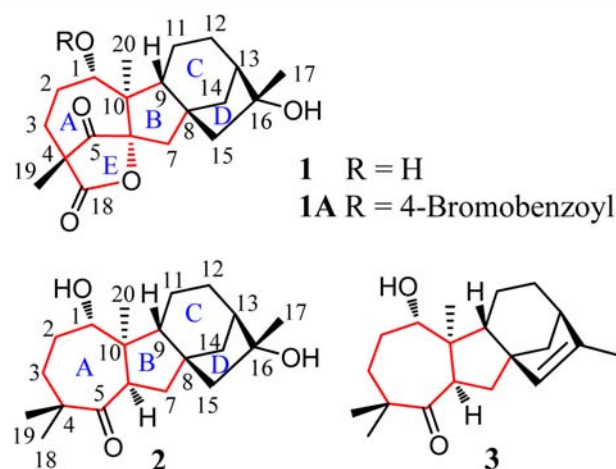


Figure 1. Structures of compounds 1, 1A, 2, and 3.

the ¹³C NMR spectrum. The ¹H NMR, together with the HSQC spectrum of 1, showed resonances attributable to three tertiary methyl groups (δ_H 1.54, 1.45, 1.34). The ¹³C NMR and DEPT spectra indicated 20 carbon resonances ascribed to three methyls, seven methylenes, three methines (one oxygenated), and seven quaternary carbons (one keto-carbonyl, one ester-carbonyl, and one oxygenated) (see Table 1). The aforementioned functionalization (one keto-carbonyl and one ester-carbonyl) accounted for two degrees of unsaturation, and the remaining five degrees of unsaturation required 1 to possess a pentacyclic ring system.

Received: January 8, 2017

Published: February 2, 2017

Table 1. NMR Data for Compounds 1–3 in C₅D₅N

no.	1 ^a		2 ^b		3 ^b	
	δ_{H} (J, Hz)	δ_{C}	δ_{H} (J, Hz)	δ_{C}	δ_{H} (J, Hz)	δ_{C}
1	3.73, dd (10.5, 5.5)	79.9	3.79, m	77.2	3.70, m	77.1
2a	2.25, overlap	31.1	2.11, overlap	30.7	2.09, overlap	30.6
2b	1.86, dt (14.5, 3.5)		2.01, m		2.01, m	
3a	1.99, dd (9.5, 4.0)	38.7	2.12, overlap	34.0	2.08, m	34.1
3b	1.75, overlap		1.44, d (9.0)		1.46, m	
4		51.6		46.1		46.1
5		212.1		218.0		218.3
6		97.2	3.25, dd (8.4, 3.0)	55.8	3.30, dd (7.8, 1.8)	55.9
7a	2.46, d (14.0)	43.6	2.50, d (13.2)	37.9	2.39, dd (13.8, 1.8)	35.4
7b	2.27, d (14.0)		1.94, dd (13.8, 8.4)		1.79, overlap	
8		45.2		50.4		53.0
9	2.08, dd (11.0, 6.5)	59.0	1.88, overlap	59.4	1.97, dd (10.8, 7.2)	50.9
10		53.4		54.4		53.7
11a	2.01, overlap	20.2	2.04, m	20.8	2.29, m	22.9
11b	1.77, m		1.87, m		2.15, m	
12a	1.74, overlap	22.6	1.73, m	24.5	1.55, m	21.5
12b	1.49, m		1.59, m		1.29, m	
13	2.19, m	47.3	2.23, overlap	47.9	2.06, m	42.1
14a	2.37, dd (11.0, 4.0)	36.3	2.38, dd (11.4, 4.2)	38.0	2.11, overlap	42.4
14b	1.77, overlap		1.80, d (10.8)		1.76, overlap	
15a	2.50, d (13.5)	60.9	2.51, d (13.2)	60.4	6.16, s	139.0
15b	2.30, d (13.8)		2.23, d (13.8)			
16		79.9		79.7		146.2
17	1.54, s	26.7	1.51, s	26.7	1.67, d (1.2)	15.3
18		175.5	0.96, s	28.5	0.95, s	28.5
19	1.34, s	16.0	1.22, s	22.1	1.20, s	21.8
20	1.45, s	10.4	1.39, s	16.4	1.32, s	15.1
1-OH	6.44, d (5.0)		5.97, d (5.4)		5.89, d (4.8)	
16-OH	5.42, s		5.38, s			

^aRecorded in C₅D₅N at 500 MHz for ¹H NMR and 125 MHz for ¹³C NMR. ^bRecorded in C₅D₅N at 600 MHz for ¹H NMR and 150 MHz for ¹³C NMR.

The planar structure of **1** was elucidated by detailed analysis of 1D and 2D NMR spectra. Further analysis of the ¹H–¹H COSY spectrum and HSQC experiment identified two structural fragments (bold in Figure 2): (a) C(1)H–

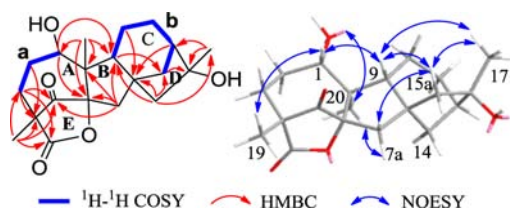


Figure 2. Key 2D NMR correlations of **1**.

C(2)H₂–C(3)H₂; (b) C(9)H–C(11)H₂–C(12)H₂–C(13)H–C(14)H₂. Fragment **b**, together with the key HMBC correlations (see Figure 2 and Figure S9) from H₂–11, H–13 to C–8 (a quaternary carbon, δ_{C} 45.2) and from H–9 to C–14 indicated that a six-membered carbon ring (ring C in Figure 2) consisted of C–8, C–9, C–11, C–12, C–13, and C–14. In addition, HMBC correlations from H₂–15 to C–8, C–9, C–13, C–14, and C–17 and from H₂–14 to C–16 revealed that a five-membered ring (ring D in Figure 2) consisted of C–13, C–14, C–8, C–15, and C–16. Rings C and D composed a bicycle[3.2.1]octane ring system. Meanwhile, HMBC correlations from a tertiary methyl (H₃–17) to C–13, C–15, and C–16 (quaternary carbon, δ_{C} 79.7)

indicated that Me–17 was connected to C–16. The aforementioned data revealed that the 6/5-fused ring system resembled those of classical *ent*-kaurane. HMBC correlations from H₃–20 to C–1, C–6, C–9, and C–10, from H₂–7 to C–6, C–8, C–9, and C–10 established that C–6, C–7, C–8, C–9, and C–10 composed another five-membered ring (ring B in Figure 2), and ring B was fused to ring C through C–8 and C–9. Furthermore, fragment **a** combined with HMBC correlations from H–1 to C–9 and C–10, from H₂–2 to C–4, from H₂–3 to C–4 and C–5, and from H₂–7 to C–5 revealed the existence of a seven-membered ring (ring A in Figure 2), which consisted of C–1, C–2, C–3, C–4, C–5, C–6, and C–10. Ring A was fused with ring B through C–6 and C–10. HMBC correlations from H₂–3 to C–18 and C–19 and from H₃–19 to C–3, C–4, C–5, and C–18 indicated that C–18 and C–19 were connected to C–4. In addition, **1** possessed a pentacyclic ring system and four rings were confirmed; there still remained one unidentified ring. Given that C–6 (a hydroxylated quaternary carbon, δ_{C} 97.2) was dramatically shifted downfield compared to a typical hydroxylated quaternary carbon and the oxygenated nature of C–18 (an ester-carbonyl, δ_{C} 175.5), a lactonic ring (ring E in Figure 2) was proposed between C–6 and C–18. Thus, the planar structure of **1** was finally established as depicted, which possessed an unusual A-homo-B-nor-*ent*-kaurane carbon skeleton with a pentacyclic 7/5/5/6/5 ring system.

The relative configuration of **1** was based on NOE difference experiments (see Figure 2 and Figures S10–S14). NOE

enhancements observed between H-1/H-9, H-1/H₃-19, H-9/H-15a, H-9/H₃-17, H-15a/H-7b, and H-15a/H₃-17 indicated that these protons were on the same face, while NOE correlation between H-7a/H₃-20 suggested that these protons were on the other side.

To further corroborate the structural assignment, we attempted to obtain a single-crystal structure of **1**. However, we found it difficult to obtain a qualified single crystal after numerous attempts. To improve its crystallinity, we modified the structure of **1** with *p*-bromobenzoyl chloride in pyridine and obtained **1A**. Fortunately, we obtained a single crystal of **1A** from acetone/water (10:1). The X-ray diffraction (Cu K α radiation) of **1A** was successfully performed [Flack parameter = $-0.03(3)$], which not only confirmed the structure assigned but also established the absolute configuration of each chiral center (1*S*,4*R*,6*S*,8*S*,9*R*,10*R*,13*R*,16*R*), as shown (see Figure 3). Crystallographic data of **1A** have been deposited at the Cambridge Crystallographic Data Centre (CCDC) (deposition no. 1526088).

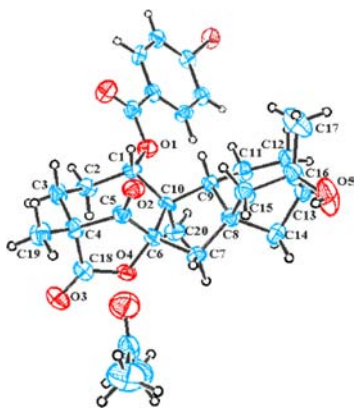


Figure 3. ORTEP drawing of **1A**.

Pierisketone B (**2**) was assigned a molecular formula of C₂₀H₃₂O₃ based on its HRESIMS ion m/z 343.2256 ($[M + Na]^+$, calcd for 343.2244), incorporating five degrees of unsaturation. The ¹H NMR spectrum showed resonances attributable to four tertiary methyls at δ_H 1.51, 1.39, 1.22, and 0.96. The ¹³C NMR data, with the aid of a DEPT spectrum, revealed the presence of four methyls, seven methylenes, four methines (one oxygenated), and five quaternary carbons (one keto-carbonyl and one oxygenated) (see Table 1). The ¹H and ¹³C NMR data of **2** were similar to those of **1**. The major differences were that **2** was found to have an additional tertiary methyl (H₃-18, δ_H 0.96; C-18, δ_C 28.5) and an additional methine (H-6, δ_H 3.25; C-6, δ_C 55.8) instead of two quaternary carbons (C-18, δ_C 175.5; C-6, δ_C 97.2) in **1**. The spin-coupling system C(6)H–C(7)H₂ identified by ¹H–¹H COSY, together with the key HMBC (see Figure 4 and Figure S22) correlations from the *gem*-dimethyl H₃-18 (H₃-19) to C-3, C-4, and C-5, verified the above deduction. Further HSQC and HMBC experiments allowed the full assignments of the ¹H and ¹³C NMR data of **2**.

In the NOESY spectrum (see Figure 4 and Figures S23–S25), cross-peaks from H-6 to H₃-18 and H₃-20 indicated that H-6, H₃-18, and H₃-20 oriented on the same side of the ring system. In addition, cross-peaks from H-1 to H-9 and H₃-19 and from H-9 to H-15a and H₃-17 revealed that these protons were oriented in another side of the ring system.

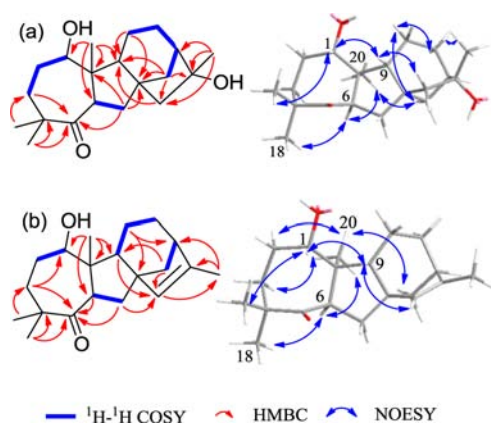


Figure 4. (a) Key 2D NMR correlations of **2**; (b) Key 2D NMR correlations of **3**.

ECD has proven to be a powerful and reliable method for determining the absolute configuration of natural products.¹⁰ To determine the absolute configuration of **2**, time-dependent density functional theory at the B3LYP/6-31G(d)¹⁰ was used by comparing the calculated ECD spectra of **2a** (1*S*,6*R*,8*S*,9*R*,10*R*,13*R*,16*R*) and its enantiomer **2b** (see Figure 5). The experimental ECD spectrum of **2** agreed perfectly with

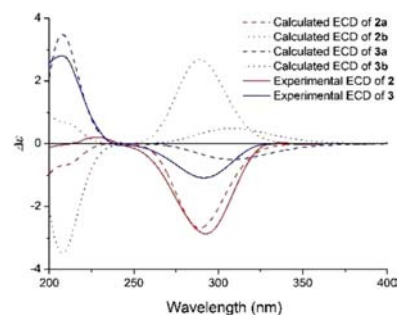


Figure 5. Experimental and calculated ECD spectra for **2** and **3**.

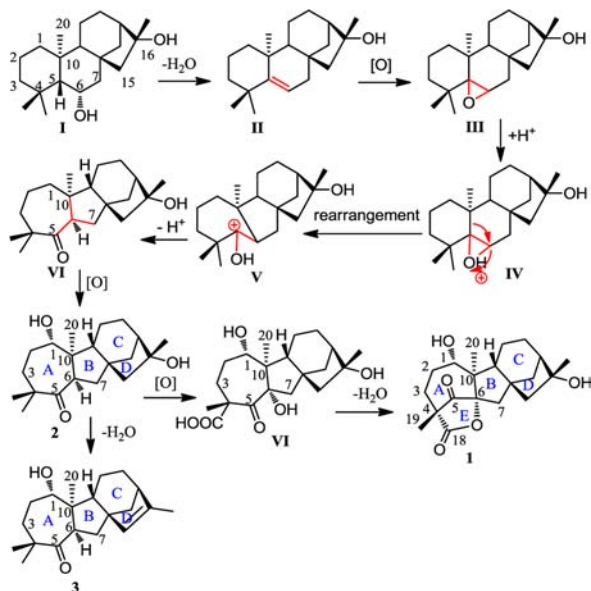
the calculated ECD spectrum of **2a**. Thus, the absolute configuration of **2** was established as depicted (1*S*,6*R*,8*S*,9*R*,10*R*,13*R*,16*R*).

Pierisketone C (**3**) gave a molecular formula of C₂₀H₃₀O₂, as determined by HRESIMS. Analysis of the molecular mass revealed that **3** was 18 mass units less than **2**. Further comparing the NMR data, it was found that the spectra of **3** closely resembled those of **2**. The only difference was that **3** was found to have an additional double bond. The key HMBC correlations (see Figure 4 and Figure S34) from H-9 and H₃-17 to C-15 (δ_C 139.0) and from H₂-12 and H₃-17 to C-16 (δ_C 146.2) established the location of the double bond at $\Delta^{15,16}$. The remaining carbons and protons were assigned by analysis of 2D NMR spectrum. NOESY correlations (see Figure 4 and Figures S35–S37) from H-6 to H₃-18 and H₃-20 revealed these protons were on the same side. NOESY correlations from H-1 to H-9 and H₃-19 and from H-9 to H-15 indicated these protons on the other side. The absolute configuration of **3** was determined by comparing the calculated ECD spectra of **3a** (1*S*,6*R*,8*S*,9*R*,10*R*,13*R*) and its enantiomer **3b** (see Figure 5) using time-dependent density functional theory at the B3LYP/6-31G(d).¹⁰ The experimental ECD spectrum of **3** was an excellent match with calculated ECD spectrum of **3a**. Thus, the

absolute configuration of **3** was established as (1*S*,6*R*,8*S*,9*R*,10*R*,13*R*).

Pierisketolide A (**1**) and pierisketones B and C (**2** and **3**) represent an unusual A-homo-B-nor-*ent*-kaurane carbon skeleton. Biosynthetically, **1**–**3** might rationally be generated from an *ent*-kaurane precursor (6 α ,16 α -dihydroxy-*ent*-kaurane, **I**),¹¹ as seen in Scheme 1. The *ent*-kaurane precursor might undergo

Scheme 1. Plausible Biosynthetic Pathways of Pierisketolide A (1**) and Pierisketones B and C (**2** and **3**)**



dehydration, epoxidation, intramolecular rearrangement, and hydroxylation to produce pierisketone B (**2**). On one hand, **2** subsequently undergoes hydroxylation to yield pierisketone C (**3**). On the other hand, **2** undergoes oxidation and dehydration to yield pierisketolide A (**1**).

Compound **1** was evaluated for analgesic activity. In the acetic acid induced writhing test, **1** exhibited an analgesic effect with a 45% writhing inhibition rate at 10.0 mg/kg compared to a blank control. As a comparison, the positive control (morphine) had a 68% writhing inhibition rate at a dose of 0.5 mg/kg. Compounds **1**–**3** were evaluated for both cytotoxicity against five human cancer cell lines (HCT-116, HepG2, BGC-823, NCI-H1650, and A2780) and neuroprotective effects against rotenone-induced injury in PC12 cells. No compounds displayed cytotoxicity or neuroprotective effects at a concentration of 10 μ M.

■ ASSOCIATED CONTENT

Supporting Information

The Supporting Information is available free of charge on the ACS Publications website at DOI: 10.1021/acs.orglett.7b00048.

Detailed experimental procedures, 1D and 2D NMR, MS, IR, ECD spectra, and X-ray crystallography data (PDF)

■ AUTHOR INFORMATION

Corresponding Authors

*E-mail: qujing@imm.ac.cn.

*E-mail: yushishan@imm.ac.cn.

ORCID

Shi-Shan Yu: 0000-0003-4608-1486

Notes

The authors declare no competing financial interest.

■ ACKNOWLEDGMENTS

This work was supported by the National Natural Science Foundation of China (No. 81673314), CAMS Innovation Fund for Medical Sciences (No. 2016-I2M-1-010), and PUMC Youth Fund (No. 333201606). We are grateful to the Department of Instrumental Analysis at our institute for the spectroscopic measurements.

■ REFERENCES

- (1) Christianson, D. W. *Science* **2007**, *316*, 60–61.
- (2) (a) Wang, W. G.; Li, X. N.; Du, X.; Wu, H. Y.; Liu, X.; Su, J.; Li, Y.; Pu, J. X.; Sun, H. D. *J. Nat. Prod.* **2012**, *75*, 1102–1107. (b) Zhao, W.; Wang, W. G.; Li, X. N.; Du, X.; Zhan, R.; Zou, J.; Li, Y.; Zhang, H. B.; He, F.; Pu, J. X.; Sun, H. D. *Chem. Commun.* **2012**, 48, 7723–7725.
- (3) (a) Liu, X.; Yang, J.; Wang, W. G.; Li, Y.; Wu, J. Z.; Pu, J. X.; Sun, H. D. *J. Nat. Prod.* **2015**, *78*, 196–201. (b) Zou, J.; Du, X.; Pang, G.; Shi, Y. M.; Wang, W. G.; Zhan, R.; Kong, L. M.; Li, X. N.; Li, Y.; Pu, J. X.; Sun, H. D. *Org. Lett.* **2012**, *14*, 3210–3213. (c) Wang, W. G.; Du, X.; Li, X. N.; Wu, H. Y.; Liu, X.; Shang, S. Z.; Zhan, R.; Liang, C. Q.; Kong, L. M.; Li, Y.; Pu, J. X.; Sun, H. D. *Org. Lett.* **2012**, *14*, 302–305. (d) Huang, S. X.; Xiao, W. L.; Li, L. M.; Li, S. H.; Zhou, Y.; Ding, L. S.; Lou, L. G.; Sun, H. D. *Org. Lett.* **2006**, *8*, 1157–1160. (e) Han, Q. B.; Cheung, S.; Tai, J.; Qiao, C. F.; Song, J. Z.; Tso, T. F.; Sun, H. D.; Xu, H. X. *Org. Lett.* **2006**, *8*, 4727–4730.
- (4) Sun, H. D.; Huang, S. X.; Han, Q. B. *Nat. Prod. Rep.* **2006**, *23*, 673–698.
- (5) Kuo, P. C.; Yang, M. L.; Hwang, T. L.; Lai, Y. Y.; Li, Y. C.; Thang, T. D.; Wu, T. S. *J. Nat. Prod.* **2013**, *76*, 230–236.
- (6) Wang, L. Q.; Chen, S. N.; Qin, G. W.; Cheng, K. F. *J. Nat. Prod.* **1998**, *61*, 1473–1475.
- (7) Chen, J. S.; Zheng, S. *Chinese Poisonous Plants*; Science: Beijing, 1987; pp 226–227.
- (8) Niu, C. S.; Li, Y.; Liu, Y. B.; Ma, S. G.; Li, L.; Qu, J.; Yu, S. S. *Tetrahedron* **2016**, *72*, 44–49.
- (9) Masutani, T.; Hamada, M.; Kawano, E.; Iwasa, J.; Kumazawa, Z.; Ueda, H. *Agric. Biol. Chem.* **1981**, *45*, 1281–1282.
- (10) (a) Berova, N.; Bari, L. D.; Pescitelli, G. *Chem. Soc. Rev.* **2007**, *36*, 914–931. (b) Pescitelli, G.; Di Bari, L.; Berova, N. *Chem. Soc. Rev.* **2011**, *40*, 4603–4625. (c) Pescitelli, G.; Di Bari, L.; Berova, N. *Chem. Soc. Rev.* **2014**, *43*, 5211–5233.
- (11) Chen, L. J.; Zhan, R.; Jiang, J. H.; Zhang, Y.; Dong, Y.; Chen, Y. G. *Nat. Prod. Res.* **2016**, *30*, 105–109.